Title

A microfluidic model of bacterial keratitis to quantify the efficacy of anti-infective compounds under flow

Author list

Lucy Urwin[1,2*], James H. R. Wheeler[3,4*], Paige A. Wolverson[2,5], Luke R. Green[2,5], Mahendra Raut[6,7], Esther Karunakaran[7], Lynda J. Partridge[8], Peter N. Monk[1], and William M. Durham[3]

*Lucy Urwin and James H. R. Wheeler contributed equally and are therefore co-first authors.

Email: Correspondence and requests for materials should be addressed to Lucy Urwin (l.urwin@sheffield.ac.uk) or to William M. Durham (w.m.durham@sheffield.ac.uk).

Affiliations

1. Division of Clinical Medicine, School of Medicine and Population Health, University of Sheffield, Sheffield, UK

2. The Florey Institute of Infection, University of Sheffield, Sheffield, UK

3. School of Mathematical and Physical Sciences, University of Sheffield, Sheffield, UK

4. Department of Clinical Infection, Microbiology and Immunology, University of Liverpool, Liverpool, UK

5. School of Clinical Dentistry, University of Sheffield, Sheffield, UK

6. Materials Science and Engineering, University of Sheffield, Sheffield, UK

7. School of Chemical, Materials, and Biological Engineering, University of Sheffield, Sheffield, UK

8. School of Biosciences, University of Sheffield, Sheffield, UK

Running headline: A microfluidic model of bacterial keratitis

Keywords: corneal infection, bacterial adhesion, heparin, *Staphylococcus aureus*, *Pseudomonas aeruginosa*

ORIGINAL UNEDITED MANUSCRIPT

Downloaded from academic.oup.com/jambio/advance-article/doi/10.1093/jambio/lxag263/9013327 by guest on 11 November 2026

© The Author(s) 2026. Published by Oxford University Press on behalf of Applied Microbiology International. This is an Open Access article distributed under the terms of the Creative Commons Attribution License (https://creativecommons.org/licenses/by/4.0/), which permits unrestricted reuse, distribution, and reproduction in any medium, provided the original work is properly cited.

Abstract

Aims

Bacterial infections of the cornea, also known as bacterial keratitis, are a major cause of blindness. The corneal surface is protected against infection by the flow of tear fluid, which displaces potential pathogens and debris. Whilst fluid flow is known to influence the behaviour of both bacterial and epithelial cells, most models of corneal infection use static conditions. Here, we develop a microfluidic model to directly visualise interactions between bacteria and human corneal epithelial cells (HCE2) in physiologically relevant flow conditions.

Methods and Results

We use high-resolution microscopy and automated image analysis to continuously quantify the rate at which *Staphylococcus aureus* (SH1000) and *Pseudomonas aeruginosa* (PAO1) adhere to HCE2 monolayers. We then use this system to investigate the effects of pre-treatment with unfractionated heparin (UFH), a putative therapeutic compound thought to inhibit bacterial adhesion. Using a traditional, well plate-based assay that lacks fluid flow, prior treatment of HCE2 monolayers with UFH significantly reduced adhesion of both species. In our microfluidic model we found that pre-treating HCE2 monolayers with UFH again sharply reduced *S. aureus* adhesion, but surprisingly, UFH pre-treatment had no effect on *P. aeruginosa* adhesion to corneal cells in the presence of fluid flow.

Conclusions

Our findings demonstrate that incorporating fluid flow into *in vitro* infection models can lead to qualitatively different outcomes when screening putative anti-adhesion therapies. These findings, obtained using two widely studied model strains, illustrate how microfluidic models of infection can offer valuable insights into how flow influences bacterial keratitis and guide the development of new treatments.

Impact Statement

This study develops a novel microfluidic assay to resolve how bacterial pathogens adhere to corneal epithelia under conditions that mimic flow within the eye. Surprisingly, we find that flow can alter bacterial-host cell interactions in a manner that can dramatically reduce the efficacy of a putative anti-adhesion drug, thus highlighting the importance of incorporating fluid flow into *in vitro* models for antimicrobial drug testing.

ORIGINAL UNEDITED MANUSCRIPT

Downloaded from academic.oup.com/jambio/advance-article/doi/10.1093/jambio/lxag263/9013327 by guest on 11 November 2026

Introduction

Bacterial keratitis is a sight-threatening infection that occurs when bacteria colonise the outermost layers of the cornea. These infections compromise the barrier integrity of the corneal epithelium and cause inflammation of the corneal stroma (Keay et al. 2006). Early symptoms include pain, redness, and excessive lacrimation but, if left untreated, these infections can lead to irreversible corneal scarring and subsequent loss of vision (Urwin et al. 2020). Two of the most common bacterial species that cause keratitis are the opportunistic pathogens, *Staphylococcus aureus* and *Pseudomonas aeruginosa* (Tan et al. 2017; Ting et al. 2021). Both of these species are designated by the World Health Organization as "high priority" pathogens due to their increasing rates of antibiotic resistance and prevalence in healthcare settings (WHO 2024).

One hurdle in the development of novel ophthalmic antimicrobials is the paucity of representative model systems for studying bacterial keratitis (Urwin et al. 2020). Previous research has relied heavily on *in vivo* infection models using live animals (Marquart 2011), *ex vivo* models that utilise whole excised corneas, most commonly from rabbits or pigs (Pinnock et al. 2017; Okurowska et al. 2020; Cheng et al. 2024) or on *in vitro* tissue culture models, where corneal cells are cultured in static multi-well plates (García et al. 2016; Putra et al. 2019; Cheng et al. 2024; Jadi et al. 2024). Whilst these models have made valuable contributions to our understanding of keratitis pathogenesis, they also have important limitations. *Ex vivo* systems preserve the complex 3D architecture of corneal tissue but have low throughput and thus have limited utility for screening libraries of putative antimicrobial compounds. On the other hand, *in vitro* models are much higher throughput but lack key features of the corneal environment.

Importantly, most *ex vivo* and *in vitro* models of bacterial keratitis do not account for the effect of fluid flow that is present *in vivo*. The corneal epithelium is exposed to the continuous flow of tear film across its surface, in addition to episodic flow that occurs during blinking. Fluid flow exerts shear stresses on the corneal epithelium and thus plays an important role in ocular defence by helping to remove foreign matter (Masterton and Ahearne 2018). Estimates of shear stress exerted on the corneal surface by fluid flow (measured as a force per unit area) vary widely, ranging from 0.05 dyn cm^{-2} (Kang et al. 2014) to 14 dyn cm^{-2} (Srinivas et al. 2002). While the shear exerted by the flow of tear fluid generally acts to detach foreign objects from the ocular surface, both mammalian and bacterial cells can also modulate

ORIGINAL UNEDITED MANUSCRIPT

Downloaded from academic.oup.com/jambio/advance-article/doi/10.1093/jambio/lxag263/9013327 by guest on 11 November 2026

their behaviour in response to hydrodynamic shear stress. For example, when exposed to shear stress, corneal epithelial cells increase expression of tight junction proteins, increase cell proliferation and migration, and alter their cytoskeletal morphology (Molladavoodi et al. 2017; Hampel et al. 2018). Many bacterial species can also actively sense and respond to fluid flow, which can in turn affect their ability to attach to surfaces and form biofilms (Claes et al. 2017; Rodesney et al. 2017; Webster et al. 2022). Thus, flow can impact how bacterial pathogens interact with the ocular surface both passively (by exerting mechanical forces) and actively (by inducing behavioural changes).

A range of different experimental devices have been used to study the effects of fluid flow on corneal cells in the absence of infecting bacteria. These include: flow chambers, where a syringe pump is used to drive flow between two glass coverslips separated by a gasket (Molladavoodi et al. 2017); rectangular microfluidic channels used in combination with a pneumatic pump (Hampel et al. 2018); and “cornea on a chip” devices where cells are cultured on a porous membrane sandwiched between the two layers of the device and flow is driven using syringe pumps (Bennet et al. 2018; Yu et al. 2022). However, an experimental system for studying the impact of fluid flow on host-pathogen interactions during bacterial keratitis has yet to be reported.

In this study, we develop a microfluidic model for studying the impact of fluid flow on bacterial keratitis that allows us to study how bacteria attach to corneal epithelial cells in the presence of flow using high-resolution, time-lapse microscopy. This system, which uses commercially available microfluidic well plates and a pressure-driven flow mediated by a computer-controlled manifold system (BioFlux 200, Cell Microsystems), allows up to 24 different experiments to be operated simultaneously. To demonstrate the potential of this model system for characterising putative anti-infective compounds, we quantified changes in bacterial adhesion when human corneal epithelial cell (HCE2) monolayers were pre-treated with unfractionated heparin (UFH). UFH is an analogue of heparan sulphate (HS), a linear polysaccharide that commonly decorates epithelial cell surfaces as part of heparan sulphate proteoglycans (HSPGs) (Sarrazin et al. 2011). HSPGs play a critical role in cell signalling but are also commonly exploited by bacteria to attach to and invade mammalian cells (Chen et al. 2008). UFH has previously been shown to inhibit bacterial attachment to mammalian cells (Hess et al. 2006; Rajas et al. 2017), including HCE2 monolayers (García et al. 2016; Green et al. 2023). Throughout this work we used two widely studied model bacterial strains, SH1000 (for *S. aureus*) and PAO1 (for *P. aeruginosa*),

ORIGINAL UNEDITED MANUSCRIPT

Downloaded from academic.oup.com/jambio/advance-article/doi/10.1093/jambio/lxag263/9013327 by guest on 11 November 2026

which constitutively express green fluorescent protein (GFP) to allow bacteria to be distinguished from epithelial cells. We first recapitulated the inhibitory effects of UFH on bacterial attachment to HCE2 cells using a traditional well plate-based static infection assay, before testing its effects in the presence of fluid flow, using our novel microfluidic model. Whilst UFH remained an effective inhibitor of *S. aureus* adhesion to HCE2 cells under flow, UFH surprisingly had no effect on *P. aeruginosa* attachment to HCE2 cells in our microfluidic model. Our findings thus demonstrate that the presence of fluid flow can fundamentally alter the outcome of *in vitro* infection assays, highlighting the importance of the mechanical environment during host-pathogen interactions.

Materials and Methods

Bacterial strains

S. aureus strain, SH1000-GFP, was kindly gifted by Professor Simon Foster (University of Sheffield). SH1000-GFP is derived from *S. aureus* RN4220 and contains the pSK5487 plasmid (Kwong et al. 2004), which confers resistance to chloramphenicol at 10 μg ml^{-1}. *P. aeruginosa* strain, PAO1-GFP, was kindly provided by Dr Mark Thomas (University of Sheffield). PAO1-GFP contains the non-mobilizable pIN25 plasmid (Vergunst et al. 2010), which confers resistance to chloramphenicol at 50 μg ml^{-1}.

Unfractionated heparin (UFH)

Unfractionated heparin (UFH; Heparin (Mucous) Injection BP 1,000 IU, from Leo Pharma) was obtained from the Royal Hallamshire Hospital Pharmacy. Each vial of UFH was used within 6 weeks from the date it was first opened.

Bacterial growth conditions

Luria agar (Oxoid Ltd.) containing chloramphenicol was used to isolate single bacterial colonies for inoculation of liquid cultures. Liquid cultures were prepared in Luria broth (LB; Oxoid Ltd.) and grown at 37°C, with constant agitation (180 rpm). For colony-forming unit measurements (CFU ml^{-1}), *S. aureus* was plated onto LB agar and incubated at 37°C for 16-18 h. *P. aeruginosa* was plated onto Columbia agar and horse blood (E&O Laboratories Ltd) and incubated at 37°C for 12-14 h.

ORIGINAL UNEDITED MANUSCRIPT

Downloaded from academic.oup.com/jambio/advance-article/doi/10.1093/jambio/lxag263/9013327 by guest on 11 November 2026

Fresh mid-log cultures were used for microfluidic experiments and static microscopy assays. Overnight cultures were diluted to an OD_{600} of 0.05 in LB and then incubated at 37°C, with constant agitation (180 rpm). Diluted *S. aureus* cultures were grown for approximately 3 h and *P. aeruginosa* cultures were grown for approximately 2.5 h, to allow bacteria to reach mid-log. Prior to infection, mid-log cultures were washed twice by centrifugation with phosphate buffered saline (PBS; Merck), at 4,000 x *g* for 5 min, and re-suspended in live cell imaging solution (LCIS; Invitrogen, ThermoFisher Scientific) or CO_2 independent media (Gibco, ThermoFisher Scientific) for longer-term experiments (**Fig. S1**).

For static CFU assays, frozen mid-log cultures of *S. aureus* were prepared using LB supplemented with 15% glycerol and stored at -80°C in 1.5 ml Eppendorf tubes. Frozen mid-log cultures were thawed on ice, washed once by centrifugation with PBS (16,000 x *g* for 3 min) and resuspended in keratinocyte serum free media (KSFM; Gibco, ThermoFisher Scientific). Fresh mid-log cultures of *P. aeruginosa* were prepared as described for microfluidic experiments except that 1 ml culture was transferred to an Eppendorf tube, washed by centrifugation at 16,000 x *g* for 3 min and then resuspended in KSFM. We elected to use frozen mid-log *S. aureus* stocks in the static CFU assays to match the protocols used in a recent publication (Green et al. 2023). We verified the CFU ml^{-1} of the inoculum at the beginning of each experiment to confirm consistency across experiments and assays.

Cell culture

The HCE2 [50.B1] human corneal epithelial cell line was purchased from ATCC (Manassas, Virginia, USA) and cells were cultured in KSFM, supplemented with 0.05 ng ml^{-1} bovine pituitary extract (ThermoFisher Scientific), 5 ng ml^{-1} epidermal growth factor (ThermoFisher Scientific), 500 ng ml^{-1} hydrocortisone (Merck) and 5 µg ml^{-1} insulin (Merck). HCE2 cells were maintained as sub-confluent monolayers in T-75 flasks (Corning) at 37°C, 5% CO_2. Prior to cell seeding, T-75 flasks were coated with fibronectin coating media and incubated at 37°C, 5% CO_2 for 16-18 h. The fibronectin coating media was prepared using 0.01 mg ml^{-1} fibronectin (Merck), 0.03 mg ml^{-1} bovine collagen type I (Advanced Biomatrix) and 0.01 mg ml^{-1} bovine serum albumin (BSA; Merck), prepared in Eagle's minimum essential medium (EMEM; BioWhittaker). Cells were passaged every 3-4 days using standard cell harvesting procedures.

ORIGINAL UNEDITED MANUSCRIPT

Downloaded from academic.oup.com/jambio/advance-article/doi/10.1093/jambio/lxag263/9013327 by guest on 11 November 2026

Growth curves

Bacterial strains were cultured overnight in LB. Overnight cultures were diluted to an OD_{600} of 0.05 using fresh LB or LCIS +/- 10 U ml^{-1} UFH. Diluted cultures were incubated at 37°C for 24 h under shaking conditions (200 rpm) and CFU ml^{-1} measurements were taken at 0, 2, 4, 6, 8 and 24 h post-inoculation by serially diluting culture aliquots in PBS and plating onto agar.

Microfluidic adhesion assays

All microfluidic experiments were performed using the BioFlux 200 system (Fluxion Biosciences) with 48-well low-shear (0-20 dyn cm^{-2}) plates with glass-bottomed microfluidic channels (product no. 910-0004; **Fig. 1**). Prior to experiments, microfluidic channels were coated with fibronectin coating media by adding 150 µl of fibronectin coating media to Well 1. Then continuous flow was initiated at a shear stress of 1 dyn cm^{-2} (corresponding to a flow rate of 82 µl h^{-1}) for 10 min. Plates were then incubated at 37°C, 5% CO_2 for 16-18 h. Excess fibronectin coating media was removed and 150 µl PBS was added to Well 2. Channels were then washed by initiating continuous flow from Well 2 at 1 dyn cm^{-2}, for 10 min. Excess PBS was removed, and all wells were washed once with 1 ml PBS.

Confluent HCE2 monolayers were harvested from T-75 flasks by trypsinization and centrifuged at 400 x *g* for 5 min. The cell pellet was resuspended in KSFM and the density was adjusted to 1.6 x 10^7 cells ml^{-1} using a haemocytometer. To inoculate microfluidic channels, excess PBS was first removed from both wells of the microfluidic device, and 30 µl cell suspension was added to Well 2. HCE2 cells were introduced into microfluidic channels via continuous flow at 5 dyn cm^{-2} (412 µl h^{-1}) for approximately 1-2 s. Excess cell suspension was removed and Well 2 was washed three times using PBS. Plates were transferred to a tissue culture incubator and incubated at 37°C, 5% CO_2 for 18-24 h, until a confluent monolayer had formed. To ensure that cells were exposed to continuous flow (and thus fresh medium) throughout this incubation period, we added 1 ml KSFM to Well 1 and 100 µl KSFM to Well 2, which generates a gravity-driven flow from Well 1 to Well 2 without the use of the BioFlux manifold/controller. The following day, microfluidic channels were inspected to confirm HCE2 confluency and continuous flow was initiated from Well 1 at 1 dyn cm^{-2} (82 µl h^{-1}) for 3 min, to remove dead and loosely adhered HCE2 cells.

We tried two separate approaches for inoculating bacteria into the channels:

ORIGINAL UNEDITED MANUSCRIPT

Downloaded from academic.oup.com/jambio/advance-article/doi/10.1093/jambio/lxag263/9013327 by guest on 11 November 2026

Our first approach inoculated bacterial cells only at the beginning of the experiment and then we followed a relatively small number of bacteria as they colonised HCE2 monolayers over an 8 h time period (**Fig. S1**). In these experiments, excess KSFM was first removed from both wells and 250 µl of CO_2 independent media was added to Well 2 and continuous flow was initiated at 1 dyn cm^{-2} (82 µl h^{-1}), 37°C for 60 min. *P. aeruginosa* PAO1-GFP inoculum was prepared from fresh mid-log cultures using CO_2 independent media at an OD_{600} of 0.10-0.12 (approx. 5.3 x 10^7 CFU ml^{-1}). We then added 500 µl of the bacterial inoculum to Well 2 and an equal volume of CO_2 independent medium was added to Well 1 to prevent gravity-driven flow. HCE2 monolayers were then infected with *P. aeruginosa* by a continuous infusion from Well 2 to Well 1 at 0.2 dyn cm^{-2} (16 µl h^{-1}) for 6 min. After 6 min, flow was paused, and plates were incubated at 37°C in static conditions for 30 min to allow bacteria to attach to the HCE2 monolayer. After 30 min, media in both wells was replaced with fresh CO_2 independent media and initial images of the infection were captured (t = 0 min). Pulsatile flow (2 seconds on, 2 seconds off) was then initiated at 1 dyn cm^{-2} (82 µl h^{-1}) for 120 min in the opposite direction to the flow used to initially inoculate the bacteria (i.e., from Well 1 to Well 2) and we imaged the device every 15 min using automated phase/ fluorescence microscopy.

Our second approach for inoculating bacteria into the channels was to continuously infuse bacteria along the channel throughout an experiment, which allowed us to observe bacterial adhesion to the HCE2 monolayer and quantify the impact of UFH pre-treatment across a 120 min time-period. HCE2 monolayers were first pre-treated with either 10 U ml^{-1} UFH (prepared in LCIS) or LCIS without UFH as a control. Briefly, excess KSFM was removed from all wells, 250 µl LCIS +/- UFH was added to Well 2 and continuous flow was initiated at 1 dyn cm^{-2} (82 µl h^{-1}), 37°C for 60 min. The bacterial inoculum was prepared from fresh mid-log cultures using LCIS at an OD_{600} of 0.03-0.04 (approximately 2.1 x 10^7 CFU ml^{-1}) for *S. aureus* SH1000-GFP or 0.10-0.12 (approximately 5.3 x 10^7 CFU ml^{-1}) for *P. aeruginosa* PAO1-GFP. Excess pre-treatment media was removed from both wells and 500 µl of the bacterial inoculum was added to Well 1. An equal volume of LCIS was added to Well 2 to prevent gravity-driven flow. Immediately prior to introducing bacteria (t = 0 min), images of the HCE2 monolayer were collected. Continuous flow was then initiated at 0.2 dyn cm^{-2} (16 µl h^{-1}) for 120 min and images were collected every 15 min using automated brightfield/ phase/ fluorescence microscopy.

ORIGINAL UNEDITED MANUSCRIPT

Downloaded from academic.oup.com/jambio/advance-article/doi/10.1093/jambio/lxag263/9013327 by guest on 11 November 2026

DAPI staining

HCE2 monolayers were fixed by adding 4% paraformaldehyde to Well 1 and applying flow at 0.5 dyn cm^{-2} (41 µl h^{-1}) for 20 min. Fixed cells were washed once with PBS, using the same conditions. HCE2 monolayers were then stained using 4′,6-diamidino-2-phenylindole (DAPI; ThermoFisher Scientific) at 300 nM. DAPI solution was added to Well 1 and flow was applied at 0.5 dyn cm^{-2} for 20 min. DAPI-stained cells were washed with PBS as described previously and imaged on the microscope. The procedure was carried out at room temperature (approx. 21°C).

Static adhesion assays

Two different static adhesion assays were used in this study – the first used CFUs to enumerate attached bacteria, following the methods used in a previous study (Green et al. 2023), whilst the second used light microscopy to quantify the number of attached bacteria and the same surface coatings/ media used in the microfluidic adhesion assays.

1. **Static assays enumerated using CFU**

HCE2 cells were seeded into 96-well tissue culture-treated plates at 40,000 cells per well (4 x 10^5 cells ml^{-1}), using KSFM, and incubated overnight at 37°C, 5% CO_2. Cells were washed once with Hanks balanced salt solution (HBSS; ThermoFisher Scientific) and incubated with 5% bovine serum albumin (BSA; Merck) for 60 min at 37°C, to reduce non-specific binding of bacteria to tissue culture plastic. Cells were washed once with PBS and pre-treated with KSFM containing 10 U ml^{-1} UFH or KSFM without UFH, for 60 min at 37°C. Pre-treatment media was then removed and cells were infected with SH1000-GFP or PAO1-GFP at a multiplicity of infection, MOI = 5 or MOI = 1, respectively. Typically, an increased MOI is used for *S. aureus* adhesion assays compared to *P. aeruginosa* due to differences in infectivity (Green et al. 2023; Jadi et al. 2024). Both the pre-treatment and bacterial inoculum were prepared using only KSFM (i.e. KSFM without the additional supplements that were used for longer term culture), and treatment was performed in technical triplicates for each biological repeat. HCE2 cells were infected with bacterial cultures for 60 min at 37°C in static conditions, before the inoculum was removed and washed with PBS four times. Infected cells were then lysed by incubating with 2% saponin (Merck) at 37°C for 20 min. Lysates were serially diluted in PBS, plated onto agar, and incubated at 37°C to enumerate CFUs.

ORIGINAL UNEDITED MANUSCRIPT

Downloaded from academic.oup.com/jambio/advance-article/doi/10.1093/jambio/lxag263/9013327 by guest on 11 November 2026

2. Static assays enumerated using light microscopy

Sterile, circular coverslips (12 mm diameter) were transferred to a 24-well plate and 250 µl fibronectin coating media was added to each well. Coated coverslips were incubated at 37°C with 5% CO_2 for 16-18 h. Prior to cell seeding, excess coating media was removed, and wells were washed once with 0.5 ml PBS. HCE2 cells were seeded onto coverslips by pipetting 50,000 cells suspended in KSFM into each well (5 x 10^4 cells ml^{-1}), and incubating overnight at 37°C, 5% CO_2. Cells were washed once with HBSS and pre-treated with 250 µl LCIS containing 10 U ml^{-1} UFH or LCIS without UFH (as a control) for 60 min at 37°C. Pre-treatment media was then removed, and cells were infected with SH1000-GFP or PAO1-GFP at MOI = 5 or MOI = 1, respectively. The infection inoculum was prepared in LCIS as described for microfluidic assays. HCE2 cells were infected for 60 min at 37°C, under static conditions, before the inoculum was removed and four PBS washes were performed. Infected cells were then fixed by incubating with 4% paraformaldehyde at room temperature (approx. 21°C) for 20 min. Paraformaldehyde was removed, wells were washed twice with PBS and Giemsa stain (Fluka) was added to each well for 20 min to stain bacterial and corneal cells. Giemsa stain was removed, wells washed four times with PBS and stained coverslips were mounted onto glass microscope slides. The fraction of HCE2 cells infected with bacteria was then enumerated using light microscopy (see next section) by manually locating one hundred HCE2 cells in different fields of view chosen at random locations on the coverslip. We then manually counted the number of HCE2 cells that had bacteria attached to them. The fraction of UFH-treated HCE2 cells infected with bacteria was then compared to that of a control with untreated HCE2 cells in each biological replicate.

Microscopy

All microfluidic experiments were imaged using a Nikon Ti-E inverted microscope with a Hamamatsu Flash 4.0 v2 camera, a CoolLED pE-4000 illuminator, Nikon Perfect Focus system and Nikon software (NIS-Elements AR v4.51.01). The Nikon 20X Plan Apochromat objective was used for brightfield and fluorescent microscopy and a Nikon 100X Plan Apochromat Phase objective and Ph3 phase ring were used for phase microscopy. GFP-labelled *S. aureus* and *P. aeruginosa* were visualised using epi-fluorescent images recorded every 15 min with an exposure time of 200 ms. To image DAPI-stained cells, epi-fluorescent images were captured with an exposure time of 300 ms. We used a custom-

ORIGINAL UNEDITED MANUSCRIPT

Downloaded from academic.oup.com/jambio/advance-article/doi/10.1093/jambio/lxag263/9013327 by guest on 11 November 2026

designed microscope incubation chamber with both heating and cooling modes (Digital Pixel Cell Viability and Microscopy Solutions, Science Park Square, Brighton, UK; http://www.digitalpixel.co.uk) to maintain a constant temperature of 37°C throughout microfluidic experiments. The static adhesion assays that were enumerated with microscopy were imaged using an Olympus BH-2 light microscope with a 100X Olympus BH-2 objective.

Image processing & analysis

To prevent non-adherent, planktonic bacteria from influencing the analysis of our microfluidic experiments (which in a static snapshot can look identical to attached bacteria), we used a pair of images collected in rapid succession at slightly different z-planes (separated by 2 μm) to distinguish static, attached cells from moving, planktonic ones. We averaged the two fluorescent images using the 'imageCalculator' tool in Fiji (Schindelin et al. 2012), to obtain a single GFP image at each 15 min timepoint. Because planktonic bacteria are transported by flow, they reside at different positions in the two consecutive images and therefore yield an average fluorescent intensity approximately half that of attached bacteria, which reside at the same position in both images. Using Fiji, we then thresholded the averaged fluorescent image to exclude the lower intensity pixels that corresponded to planktonic bacteria. We then segmented the resulting fluorescent images to quantify the number of attached cells using FAST (Feature-Assisted Segmenter/Tracker; (Meacock and Durham 2023)). Two separate fields of view were imaged in each microfluidic channel, and we aggregated the data from both together in our analyses.

Statistics

All statistical analysis was performed using GraphPad Prism version 9.0. For all experiments where statistical analysis is performed, we conducted four biological repeats (n = 4). Details of all statistical tests are outlined in the figure legends.

Results

Culturing HCE2 monolayers under continuous flow. We used a pressure-driven, well plate-based microfluidic system (BioFlux 200, Cell Microsystems) to culture the HCE2 corneal epithelial cell line in the presence of flow (**Fig. 1A**, **B, D**). Each plate contains 48 separate wells that are connected in pairs

ORIGINAL UNEDITED MANUSCRIPT

Downloaded from academic.oup.com/jambio/advance-article/doi/10.1093/jambio/lxag263/9013327 by guest on 11 November 2026

(denoted 'Well 1' and 'Well 2') to 24 separate microfluidic channels. The central test section of the channel is 350 μm by 75 μm in cross section (width by depth) and 4 mm in length. Well 1 is connected to the central test channel via a long serpentine channel (~200 mm in length), whereas Well 2 is connected to the opposite end of the test section via a much shorter channel (~10 mm in length, **Fig. 1B**). Flow is driven through the channels via a manifold that bolts to the top of the well plate and can drive flow in either direction through the channels via a computer-controlled pump that regulates the pressure in each well.

We first coated the interior glass surfaces of the microfluidic channels with fibronectin (**Fig. 1D**), which contains extracellular matrix proteins required for HCE2 cells to form monolayers on the untreated glass surfaces of the microfluidic devices. Fibronectin media was passed from Well 1 to Well 2 for 10 min, at a flow rate corresponding to 1 dyn cm^{-2} and the device was incubated at 37°C for 16-18 h. The following day, we removed excess fibronectin coating media from the device by flushing the channels with phosphate buffered saline (PBS). Next, we added 30 μl of HCE2 cell suspension (1.6 x 10^7 cells ml^{-1}, prepared in Keratinocyte Serum Free Media, or 'KSFM') to Well 2 and infused cells through the device for 1-2 s at a flow rate corresponding to 5 dyn cm^{-2}. Although the entire length of the device was coated with fibronectin, this protocol ensured that HCE2 cells were not inoculated into the long, narrower serpentine section (**Fig. 1B**), as preliminary experiments showed that this could block flow at later timepoints. The device containing HCE2 cells was then transferred to a tissue culture incubator for 18-24 h, where HCE2 cells proliferated to form confluent HCE2 monolayers. Following the initial incubation period, loosely attached cells were flushed out of the test channel by infusing the media through Well 1 for 3 min (1 dyn cm^{-2}) and were subsequently removed from Well 2 using a pipette. The device was then transferred to an inverted microscope (Nikon Ti-E) fitted with a temperature-controlled incubation chamber (Digital Pixel Cell Viability and Microscopy Solutions) where the confluent HCE2 monolayers were imaged continuously for the remainder of the experiment (**Fig. 1C**).

Measuring bacterial adhesion to HCE2 monolayers under continuous flow. Having established confluent HCE2 monolayers, we inoculated bacteria into the device to follow the initial stages of bacterial attachment and infection. In our microfluidic assays, bacteria can either be introduced into the channel only at the beginning of the experiment or continuously infused along the channel throughout

ORIGINAL UNEDITED MANUSCRIPT

Downloaded from academic.oup.com/jambio/advance-article/doi/10.1093/jambio/lxag263/9013327 by guest on 11 November 2026

the experiment. The former approach was tested initially, allowing us to follow a relatively small number of inoculated bacteria as each individual bacterium proliferates clonally on the surface of the HCE2 monolayers over an 8 h infection period (**Fig. S1**). However, because of our interest in anti-adhesion therapies we ultimately chose to focus on the first 120 min of bacterial infection, allowing us to directly quantify the rate at which individual bacterial cells adhere to the corneal surface. To this end, for the remainder of the study, we continuously infused bacterial cells over HCE2 monolayers to follow the temporal dynamics of initial bacterial attachment (**Fig. 1D**).

Both bacterial strains that we studied were engineered to constitutively express GFP (Kwong et al. 2004; Vergunst et al. 2010), which allowed them to be readily distinguished from epithelial cell monolayers. However, since HCE2 cells do produce a weak signal in the GFP channel, each of our experiments started by recording an image of HCE2 cells in the absence of any bacterial cells (at $t = 0$) to establish a baseline and ensure that HCE2 cells were not misidentified as bacteria in subsequent analyses. We then added 500 µl of either *S. aureus* (SH1000-GFP) or *P. aeruginosa* (PAO1-GFP) inoculum to Well 1 and began infusing bacteria (0.2 dyn cm^{-2}) over the monolayer of HCE2 cells. We imaged brightfield and GFP signal at 15 min intervals in two separate fields of view in the test section of each channel. We then used automated image analysis software (the Feature Assisted Segmenter-Tracker, or 'FAST' (Meacock and Durham 2023)) to segment individual bacterial cells attaching to the HCE2 monolayer and measure the density of bacterial cells on the surface of the corneal epithelial cells at each timepoint. This analysis pipeline allowed us to distinguish each individual bacterial cell at later timepoints in the experiment, even those residing in close proximity to one another (**Fig. 2A, B**).

One of the main control variables in static *in vitro* infection models is the multiplicity of infection (MOI). This metric describes the ratio of bacterial to host cells at the start of static infection assays and is a key determinant of infection outcome. However, it is not straightforward to calculate MOI in microfluidic systems for a number of reasons: firstly, only a fraction of the bacteria introduced into the inlet well of the microfluidic device actually reach the test channel; secondly, the number of bacteria that encounter each HCE2 cell increases over time as bacteria continuously pass through the channel; and finally, our time-lapse images only quantify attached bacteria, not the ones that remain suspended in the bulk flow. However, we can quantify a dynamic metric that estimates how the number of bacteria attached to each

ORIGINAL UNEDITED MANUSCRIPT

Downloaded from academic.oup.com/jambio/advance-article/doi/10.1093/jambio/lxag263/9013327 by guest on 11 November 2026

HCE2 cell changes over time. To calculate this, we measured the average density of HCE2 cells in our microfluidic devices by using DAPI (4′,6-diamidino-2-phenylindole) to stain HCE2 nuclei, and then used image-processing software to segment and quantify the number of stained nuclei (**Fig. 2C**, **Fig. S2**, (Meacock and Durham 2023)). We found a mean of approximately 1100 HCE2 nuclei per mm^2 in the test section, which is expected to remain relatively constant over the course of a two-hour experiment. We estimate that the number of attached bacteria per HCE2 cell increases from zero at the beginning of the experiment to approximately three after 60 min for both *S. aureus* and *P. aeruginosa* (**Fig. S2**). The rate of attachment then slows down in the case of *P. aeruginosa*, increasing to approximately four bacteria per HCE2 cell after 120 min, perhaps suggesting that the sites at which *P. aeruginosa* can attach to HCE2 cells may begin to saturate in the latter stages of the experiment. In the case of *S. aureus*, a slow-down in the rate of attachment is not evident and on average approximately six bacteria are attached to each HCE2 cell after 120 min.

UFH pre-treatment leads to a significant reduction in *S. aureus* adhesion to HCE2 monolayers under continuous flow conditions. Before using our microfluidic assay to test how UFH affects the ability of *S. aureus* to attach to HCE2 cells under flow, we first repeated a microtiter plate assay (Green et al. 2023) that quantifies bacterial attachment in static conditions (**Fig. S3B**) using our GFP-tagged *S. aureus* strain, SH1000-GFP. Briefly, HCE2 cells were cultured in 96-well plates, incubated with 5% bovine serum albumin to block non-specific bacterial binding and treated with 10 U ml^{-1} UFH for 60 min. The UFH was then removed, and HCE2 monolayers were infected with *S. aureus* (MOI = 5) for 60 min under static conditions. The infected cells were washed four times with PBS to remove loosely adhered bacteria and then lysed with 2% saponin. The mixture of lysed HCE2 cells and bacteria was then plated onto agar to measure colony-forming units (CFU). In line with previous work (Green et al. 2023), we found that under these static conditions, pre-treating HCE2 cells with UFH reduced the number of adherent *S. aureus* (SH1000-GFP) by 49% (**Fig. 3E**).

We next tested if pre-treatment with UFH had a similar effect in our microfluidic assay, where bacteria instead attach under continuous flow. We cultured HCE2 monolayers in two adjacent microfluidic channels within the same device. We then passed 10 U ml^{-1} UFH (prepared in live cell imaging solution, or ‘LCIS’) through one channel and LCIS-only control (containing no UFH) through the other channel

ORIGINAL UNEDITED MANUSCRIPT

Downloaded from academic.oup.com/jambio/advance-article/doi/10.1093/jambio/lxag263/9013327 by guest on 11 November 2026

414 for 60 min. After 60 min, excess LCIS was removed from the wells and *S. aureus* (SH1000-GFP)
415 infection inoculum was infused continuously through both channels (at a shear stress of 0.2 dyn cm^{-2}),
416 allowing us to compare the rate of bacterial attachment to HCE2 cells pre-treated with UFH and control
417 HCE2 monolayers that were not treated with UFH.
418
419 Our initial inspection of the time-lapse microscopy images suggested that, as in static conditions, *S.*
420 *aureus* bacteria displayed dramatically reduced adhesion to UFH-treated HCE2 cells compared to
421 untreated HCE2 monolayers (**Fig. 3A**). However, to ensure that these observations did not depend on
422 the specific z-plane that was being imaged, we also collected a z-stack of 15 images equally spaced
423 over a range of 28 μm at *t* = 120 min post-infection (**Fig. S4A**) and calculated the maximum intensity
424 projection across all z-planes (**Fig. 3B**). This analysis confirmed that *S. aureus* attachment to HCE2
425 monolayers was reduced following UFH pre-treatment and did not simply result from an imaging artefact
426 (**Fig. 3B**).
427
428 While the difference between the UFH and control treatments is readily observable by eye (**Fig. 3A**),
429 we used automated image analysis to identify individual *S. aureus* cells attached to the HCE2
430 monolayer and quantified their numerical density at each time-point (**Fig. 3C**, **Fig. S5**). This analysis
431 showed that the number of attached *S. aureus* bacteria per unit area increased steadily in both control
432 and UFH conditions for the first 30 min post-infection, with only small differences between the two
433 treatments. However, from 45-120 min post-infection, attachment to the UFH-treated cells started to
434 plateau whereas bacteria continued to attach to HCE2 cells in the untreated control at approximately
435 the same rate. Indeed, we observed a statistically significant reduction in the number of *S. aureus*
436 bacteria attached to the UFH-treated HCE2 monolayer at each timepoint between 60 and 120 min post-
437 infection (**Fig. S5**), with a 65% reduction in bacterial adhesion to UFH-treated HCE2 monolayers by 60
438 min post-infection (**Fig. 3D**). A similar trend was observed when the optical density of the bacterial
439 inoculum was increased by approximately four-fold (**Fig. S6**). To test whether our findings could be
440 affected by changes in the growth rate of the bacteria induced by UFH, we conducted separate
441 experiments to directly compare the growth of *S. aureus* in the presence and absence of 10 U ml^{-1} UFH.
442 These experiments confirmed that UFH had no appreciable effect on the growth of *S. aureus*,
443 regardless of whether bacteria were cultured in the nutrient-limited LCIS used for microfluidic assays,

ORIGINAL UNEDITED MANUSCRIPT

Downloaded from academic.oup.com/jambio/advance-article/doi/10.1093/jambio/lxag263/9013327 by guest on 11 November 2026

or in nutrient-rich LB (**Fig. S7A**). Our results support the hypothesis that reduced numbers of *S. aureus* cells observed on UFH-treated HCE2 monolayers were driven by differences in the bacterial attachment rate.

We next sought to confirm whether differences in attachment could be driven by non-specific effects of UFH treatment on bacterial adhesion that might also occur in the absence of corneal cells. To this end, we measured how UFH pre-treatment affected the attachment of *S. aureus* to the glass surface of our microfluidic device in the absence of HCE2 cells (**Fig. S8A** and **B**). Two adjacent channels were coated with fibronectin and then one of the two channels was pre-treated with LCIS containing 10 U ml^{-1} UFH for 60 min, whilst the other was exposed to LCIS without UFH as a control. *S. aureus* was then continuously infused through both channels, as previously described. *S. aureus* cells were observed to readily attach to fibronectin-coated glass, however, the number of surface-attached *S. aureus* at 120 min (**Fig. S8B**) was consistently lower than bacterial attachment to HCE2 monolayers under equivalent inoculation conditions (**Fig. 3C**). Importantly, we did not observe any appreciable differences in bacterial adhesion to the glass surface of our devices when comparing channels with and without UFH pre-treatment (**Fig. S8A** and **B**). This suggests that the reduction in *S. aureus* attachment observed for HCE2 monolayers pre-treated with UFH is driven by changes in the mammalian cell surface, rather than a generic, non-specific effect of UFH on bacterial adhesion.

Taken together, these results suggest that UFH pre-treatment inhibits the attachment of *S. aureus* to HCE2 monolayers both in the presence and absence of fluid flow. Furthermore, the mechanism by which UFH reduces bacterial adhesion appears to be host-directed, as inhibitory effects are not observed in the absence of HCE2 monolayers and UFH has no direct effects on *S. aureus* growth.

The effect of UFH pre-treatment on *P. aeruginosa* adhesion to HCE2 monolayers is contingent on fluid flow. Given the efficacy of UFH pre-treatment in inhibiting the attachment of *S. aureus* to corneal epithelial cells, we decided to test whether this compound could also inhibit the attachment of *P. aeruginosa*, another major causative agent of bacterial keratitis. We first tested UFH pre-treatment using the static infection assay shown in **Fig. 3E** and observed that, as for *S. aureus*, UFH pre-treatment significantly reduces *P. aeruginosa* attachment to HCE2 monolayers in static conditions (**Fig. 4E**).

ORIGINAL UNEDITED MANUSCRIPT

Downloaded from academic.oup.com/jambio/advance-article/doi/10.1093/jambio/lxag263/9013327 by guest on 11 November 2026

We next sought to test whether UFH pre-treatment reduces *P. aeruginosa* attachment in the presence of fluid flow. From our experiments with *S. aureus*, we hypothesised that fluid flow was unlikely to influence the efficacy of UFH pre-treatment (**Fig. 3**). To test this hypothesis, we repeated the experiment shown in **Fig. 3**, but this time using the *P. aeruginosa* strain, PAO1-GFP, as our infective agent. Contrary to our predictions, time-lapse and z-stack images appeared to show similar numbers of *P. aeruginosa* bacteria attached to both UFH-treated and untreated HCE2 monolayers (**Fig. 4A, 4B** and **S4B**). To confirm these initial observations, the number of attached *P. aeruginosa* bacteria per unit area was calculated at 15 min increments from t = 0 to 120 min post-infection (**Fig. 4C**). The resulting bacterial cell densities were statistically indistinguishable at every timepoint for untreated compared to UFH-treated HCE2 monolayers (**Fig. S9**) and at 60 min post-infection, no reduction in bacterial attachment was observed (**Fig. 4D**).

Given this unexpected result, we sought to determine if the lack of UFH-mediated inhibition in our microfluidic assay was due to the presence of fluid flow or if it could be attributed to other differences between the microfluidic and static adhesion assays (**Fig. S3**), briefly summarised here. Firstly, the two assays used plates with different surface properties - our static adhesion assays used tissue-culture treated polystyrene well plates, whilst our microfluidic experiments used fibronectin coated glass surfaces. Secondly, the bacterial inoculum was prepared in KSFM media for static adhesion assays, whereas LCIS was used for the microfluidic plate format. Thirdly, the original static assay included a pre-incubation step with 5% bovine serum albumin (BSA) to block non-specific bacterial binding to tissue-culture plastic; however, BSA was not used in the microfluidic assay. Finally, the two assays utilised different techniques to enumerate attached bacterial cells. In static assays, infected HCE2 monolayers were first washed with PBS to remove any non-adherent bacterial cells before being lysed with saponin and plated onto agar to measure CFUs. In contrast, in our microfluidic assays, we enumerated attached bacteria directly using microscopy. The difference in UFH pre-treatment efficacy observed between our static and microfluidic assays for *P. aeruginosa* could thus be caused by the effects of fluid flow or these other differences between the two assays.

ORIGINAL UNEDITED MANUSCRIPT

Downloaded from academic.oup.com/jambio/advance-article/doi/10.1093/jambio/lxag263/9013327 by guest on 11 November 2026

To distinguish between these possibilities, we designed an alternative protocol for measuring bacterial adhesion under static conditions that more closely mimicked our microfluidic assays and utilised light microscopy to enumerate adherent bacteria (**Fig. S3C**). Briefly, HCE2 cells were seeded onto glass coverslips in a 24-well plate that had first been coated with fibronectin coating media. These HCE2 cells were then either pre-treated with LCIS media containing 10 U ml^{-1} UFH for 60 min or LCIS media without UFH. HCE2 cells were then infected with either *S. aureus* or *P. aeruginosa* prepared in LCIS. After 60 min, non-adherent and loosely-attached bacteria were removed by washing with PBS, the infected cells were fixed with 4% paraformaldehyde and stained with Giemsa. As in our microfluidic assays, BSA was not used and we used light microscopy to directly enumerate adherent bacteria. Specifically, for each of our four biological repeats, one hundred HCE2 cells were analysed directly using light microscopy across multiple fields-of-view. To quantify how UFH pre-treatment affects bacterial attachment, we measured the proportion of HCE2 cells that had bacteria attached to them. Importantly, this method allowed us to distinguish bacteria directly attached to HCE2 cells from bacteria non-specifically attached to the fibronectin-coated glass coverslips. We found that UFH pre-treatment in this static assay led to an over 40% reduction in both *S. aureus* and *P. aeruginosa* adhesion to HCE2 monolayers (**Fig. S10**). This result, combined with those from our microfluidic assays and the CFU-based static attachment assay (all summarised in **Fig. S10**), suggests that flow plays a critical role in influencing UFH-mediated inhibition of *P. aeruginosa* attachment to HCE2 cells.

Finally, we note that, as with *S. aureus*, UFH had no appreciable effect on the growth of *P. aeruginosa* when cultured in either LCIS or nutrient-rich LB (**Fig. S7B**). We also observed that in the absence of HCE2 cells, UFH pre-treatment of fibronectin-coated microfluidic channels had no appreciable effect on *P. aeruginosa* attachment relative to untreated fibronectin coated glass (**Fig. S8A** and **C**). Thus, as with *S. aureus*, UFH does not appear to have a generic, non-specific effect on *P. aeruginosa* attachment to abiotic surfaces.

Discussion

Flow is a ubiquitous feature of the corneal surface and is known to affect the behaviour of corneal epithelial cells (Molladavoodi et al. 2017; Hampel et al. 2018) and the pathogens that infect them (Claes

ORIGINAL UNEDITED MANUSCRIPT

Downloaded from academic.oup.com/jambio/advance-article/doi/10.1093/jambio/lxag263/9013327 by guest on 11 November 2026

et al. 2017; Rodesney et al. 2017; Webster et al. 2022). However, experimental models for studying bacterial keratitis are predominantly conducted in static conditions. Here, we establish a protocol for infecting HCE2 monolayers with common causative agents of bacterial keratitis (**Fig. 1**) in the presence of flow-induced shear stresses that are within the predicted range for the ocular surface (Srinivas et al. 2002; Kang et al. 2014). We visualised the earliest stages of the infection process (**Fig. 2**) and quantified bacterial attachment to HCE2 monolayers using a combination of time-lapse fluorescent microscopy and automated image analysis (**Figs. 3** and **4**). We then investigated how fluid flow affects the efficacy of UFH by comparing the results from the microfluidic assay with those from classical well plate-based assays where bacteria instead attach under static conditions.

UFH has been previously shown to inhibit the adhesion of diverse bacterial species to mammalian cells in static conditions (Rajas et al. 2017), including HCE2 monolayers (García et al. 2016; Green et al. 2023). We recapitulated these results for *S. aureus* and *P. aeruginosa* using a previously established static assay that uses 96-well plates and CFU-based measurements to quantify bacterial adhesion to HCE2 cells (**Figs. 3E** and **4E**). We found that UFH pre-treatment reduces *S. aureus* attachment to HCE2 monolayers in both our static and microfluidic infection models, suggesting that fluid flow does not affect UFH-mediated adhesion inhibition for this bacterial species (**Fig. 3)**. In contrast, we observed that the efficacy of UFH on *P. aeruginosa* attachment was flow dependent – we observed UFH pre-treatment reduced *P. aeruginosa* attachment to corneal cells in the static assay but did not affect adhesion when exposed to the continuous flow in our microfluidic assay (**Fig. 4**). To test if these different outcomes might result from other experimental factors, we then performed an additional static assay that used the same surface coating and media as used in our microfluidic assays, as well as using microscopy to enumerate bacterial attachment (**Fig. S3C**). We again observed that UFH reduced both *S. aureus* and *P. aeruginosa* adhesion to HCE2 monolayers (**Fig. S10**) in the alternative static assay (which more closely approximates our microfluidic system). Taken together, our results indicate that flow does not affect UFH's ability to inhibit *S. aureus* adhesion to corneal cells, but that UFH-mediated inhibition of *P. aeruginosa* adhesion occurs only in the absence of fluid flow. However, future work will be required to determine how broadly our findings are conserved beyond the widely used model bacterial strains (SH1000 and PAO1) and corneal epithelial cell line (HCE2) used in this study. For example, future experiments using clinical bacterial isolates and primary corneal epithelial cultures may shed light on the generality of the flow-dependent effects reported here.

Downloaded from academic.oup.com/jambio/advance-article/doi/10.1093/jambio/lxag263/9013327 by guest on 11 November 2026

Our results suggest a complex interplay between host, pathogen, and fluid flow, raising important questions about why UFH pre-treatment has differential effects on *S. aureus* and *P. aeruginosa* attachment in the presence of flow. Previous studies involving static infection models have identified a mechanism for UFH-mediated inhibition of *S. aureus*; it was found that UFH prevents staphylococcal adhesion by triggering the reorganisation of two membrane-anchored receptors – α5β1 integrin and the heparan sulphate proteoglycan (HSPG) syndecan-1 – at the host cell surface (Green et al. 2023). Less is known about UFH-mediated inhibition of *P. aeruginosa* attachment and the specific importance of α5β1 and syndecan-1 has not been confirmed, but the sulphate moieties of HSPGs have previously been shown to act as binding platforms for *P. aeruginosa*, via an interaction that is blocked by heparin (Bucior et al. 2010). Furthermore, *P. aeruginosa* has previously been shown to induce syndecan-1 shedding both *in vitro* (Park et al. 2000) and *in vivo* (Park et al. 2001). It should also be noted that HSPGs display remarkable heterogeneity in structure, ligand-specificity and localisation, with some HSPGs anchored to the host cell surface and others secreted into the host extracellular matrix (Sarrazin et al. 2011). Therefore, one possibility is that under static conditions, *P. aeruginosa* preferentially interacts with non-anchored HSPGs or shed HSPG ectodomains via an interaction that is blocked by UFH. In contrast, in the presence of flow, non-anchored HSPGs and shed HSPG ectodomains may be displaced from the corneal cell surface, causing *P. aeruginosa* to instead utilise alternative host binding sites that are not sensitive to UFH pre-treatment.

Alternatively, flow could potentially trigger a phenotypic switch in *P. aeruginosa* that favours the use of an alternative binding mechanism. Consistent with this idea, previous work has shown that *P. aeruginosa* can actively sense and respond to flow (Rodesney et al. 2017; Sanfilippo et al. 2019). Fluid flow alters intracellular levels of the global bacterial second messenger, cyclic-di-GMP, in surface-attached *P. aeruginosa* (Rodesney et al. 2017), which in turn regulates a range of physiological and behavioural processes associated with biofilm formation. Intriguingly, *P. aeruginosa* also regulates gene expression in response to changes in ambient flow speed, rather than the forces exerted by flow, which also depend on the fluid viscosity (Sanfilippo et al. 2019). In addition, the residence time of *P. aeruginosa* on abiotic surfaces has been shown to increase with increasing shear stress (Lecuyer et al. 2011; Palalay et al. 2023). Therefore, flow may stimulate *P. aeruginosa* cells to increase their residence time on the corneal surface, potentially allowing these bacteria to form secondary host-cell interactions that are not disrupted by UFH pre-treatment. While many processes are involved in *P. aeruginosa*

Downloaded from academic.oup.com/jambio/advance-article/doi/10.1093/jambio/lxag263/9013327 by guest on 11 November 2026

infections of the cornea (Evans and Fleiszig 2013), our results clearly highlight how flow can affect bacterial attachment to corneal cells and the efficacy of putative drugs used to inhibit this process.

It is important to note that *P. aeruginosa* is the leading causative agent of contact lens-associated keratitis (Fleiszig et al. 2020) and fluid flow beneath soft contact lenses is driven by contact lens deformation during blinking rather than by direct eyelid sweep (Maki and Ross 2014). Whether UFH or other drugs might inhibit *P. aeruginosa* adhesion in this mechanically complex flow environment remains undetermined and warrants further study. For example, future work incorporating a contact lens surface and lens-specific flow conditions into a microfluidic device could guide the development of anti-adhesion strategies specifically targeted at contact lens-associated keratitis.

Previous studies have developed microfluidic models to understand how bacteria infect non-ocular human tissues. For instance, microfluidic models have been used to study how *Escherichia coli* infects the intestine (Kim et al. 2010; Alsharif et al. 2015; Tremblay et al. 2015; Pedersen et al. 2018), and how *S. aureus* (Pedersen et al. 2018) and *Neisseria meningitidis* (Mairey et al. 2006) infect endothelial cells. However, directly resolving the effect of fluid flow on initial bacterial attachment has remained elusive, as previous microfluidic models have either infected mammalian cells in static conditions (before introducing flow at later timepoints) (Kim et al. 2010; Alsharif et al. 2015; Tremblay et al. 2015) or used fixed mammalian cells that cannot respond to flow (Pedersen et al. 2018). Therefore, we envisage that our microfluidic assay could also be used to study how fluid flow affects the initial stages of infection at other sites within the body.

Static, well plate-based assays are intrinsically high-throughput. However, they lack physiologically relevant flow conditions, are operated in “batch” so that the chemical environment changes over time as nutrients are consumed and waste products are produced, and typically only provide a single CFU measurement as a readout. By contrast, microfluidic assays are lower throughput, but they can be used to study infection in the presence of flow, allow the chemical environment to be maintained consistently over time, and facilitate live cell imaging to directly visualise the dynamics over time. The assay described here allows up to 24 different experiments to be conducted in parallel, which allows these assays to simultaneously test a relatively large number of compounds or different genotypes in identical conditions. When combined with automated image analysis, these microfluidic assays open new

Downloaded from academic.oup.com/jambio/advance-article/doi/10.1093/jambio/lxag263/9013327 by guest on 11 November 2026

avenues for both understanding the strategies that bacteria use to infect host cells and the development of novel therapeutics to thwart bacterial infection.

Acknowledgements

This study was funded by the Human Frontier Science Program (RGY0080/2021), the EPSRC Pump Priming Award (EP/M027430/1) and the BBSRC New Investigator Grant (BB/R018383/1). PW was supported by the Humane Research Trust (173280). Preliminary work was funded by an MRC/DPFS award (MR/S004688/1). Additional consumables were purchased using the COVID 19 Grant Extension Allocation (EP/V520469/1) from the University of Sheffield. We thank both Simon Foster and Mark Thomas at the University of Sheffield for providing bacterial strains.

Conflict of Interest Statement

The authors declare no conflicts of interest.

Data Availability Statement

The data supporting this article is available at: https://doi.org/10.15131/shef.data.34441572

Ethical approval

This article does not contain any animal experiments or studies with human participants.

ORIGINAL UNEDITED MANUSCRIPT

Downloaded from academic.oup.com/jambio/advance-article/doi/10.1093/jambio/lxag263/9013327 by guest on 11 November 2026

References

Alsharif, G., Ahmad, S., Islam, M.S., Shah, R., Busby, S.J. and Krachler, A.M. (2015) Host attachment and fluid shear are integrated into a mechanical signal regulating virulence in *Escherichia coli* O157:H7. *Proc Natl Acad Sci U S A* **112**, 5503-5508.

Bennet, D., Estlack, Z., Reid, T. and Kim, J. (2018) A microengineered human corneal epithelium-on-a-chip for eye drops mass transport evaluation. *Lab Chip* **18**, 1539-1551.

Bucior, I., Mostov, K. and Engel, J.N. (2010) *Pseudomonas aeruginosa*-Mediated Damage Requires Distinct Receptors at the Apical and Basolateral Surfaces of the Polarized Epithelium. *Infect Immun* **78**, 939-953.

Chen, Y., Götte, M., Liu, J. and Park, P.W. (2008) Microbial subversion of heparan sulfate proteoglycans. *Mol Cells* **26**, 415-426.

Cheng, K.K.W., Fingerhut, L., Duncan, S., Prajna, N.V., Rossi, A.G. and Mills, B. (2024) *In vitro* and *ex vivo* models of microbial keratitis: Present and future. *Prog Retin Eye Res* **102**, 101287.

Claes, J., Liesenborghs, L., Peetermans, M., Veloso, T.R., Missiakas, D., Schneewind, O., Mancini, S., Entenza, J.M., Hoylaerts, M.F., Heying, R., Verhamme, P. and Vanassche, T. (2017) Clumping factor A, von Willebrand factor-binding protein and von Willebrand factor anchor *Staphylococcus aureus* to the vessel wall. *J Thromb Haemost* **15**, 1009-1019.

Evans, D.J. and Fleiszig, S.M.J. (2013) Why Does the Healthy Cornea Resist *Pseudomonas aeruginosa* Infection? *Am J Ophthalmol* **155**, 961–970.e962.

Fleiszig, S.M.J., Kroken, A.R., Nieto, V., Grosser, M.R., Wan, S.J., Metruccio, M.M.E. and Evans, D.J. (2020) Contact lens-related corneal infection: Intrinsic resistance and its compromise. *Prog Retin Eye Res* **76**, 100804.

García, B., Merayo-Lloves, J., Rodríguez, D., Alcalde, I., García-Suárez, O., Alfonso, J.F., Baamonde, B., Fernández-Vega, A., Vazquez, F. and Quirós, L.M. (2016) Different Use of Cell

ORIGINAL UNEDITED MANUSCRIPT

Downloaded from academic.oup.com/jambio/advance-article/doi/10.1093/jambio/lxag263/9013327 by guest on 11 November 2026

Surface Glycosaminoglycans As Adherence Receptors to Corneal Cells by Gram Positive and Gram Negative Pathogens. *Front Cell Infect Microbiol* **6**, 173.

Green, L.R., Issa, R., Albaldi, F., Urwin, L., Thompson, R., Khalid, H., Turner, C.E., Ciani, B., Partridge, L.J. and Monk Peter, N. (2023) CD9 co-operation with syndecan-1 is required for a major staphylococcal adhesion pathway. *mBio* **14**, e01482-23.

Hampel, U., Garreis, F., Burgemeister, F., Eßel, N. and Paulsen, F. (2018) Effect of intermittent shear stress on corneal epithelial cells using an *in vitro* flow culture model. *Ocul Surf* **16**, 341-351.

Hess, D.J., Henry-Stanley, M.J., Erlandsen, S.L. and Wells, C.L. (2006) Heparan sulfate proteoglycans mediate *Staphylococcus aureus* interactions with intestinal epithelium. *Med Microbiol Immunol* **195**, 133-141.

Jadi, P.K., Dave, A., Issa, R., Tabbasum, K., Okurowska, K., Samarth, A., Urwin, L., Green, L.R., Partridge, L.J., MacNeil, S., Garg, P., Monk, P.N. and Roy, S. (2024) Tetraspanin CD9-derived peptides inhibit *Pseudomonas aeruginosa* corneal infection and aid in wound healing of corneal epithelial cells. *Ocul Surf* **32**, 211-218.

Kang, Y.G., Shin, J.W., Park, S.H., Oh, M.-J., Park, H.S., Shin, J.-W. and Kim, S.-H. (2014) Effects of Flow-Induced Shear Stress on Limbal Epithelial Stem Cell Growth and Enrichment. *PLoS One* **9**, e93023.

Keay, L., Edwards, K., Naduvilath, T., Taylor, H.R., Snibson, G.R., Forde, K. and Stapleton, F. (2006) Microbial Keratitis: Predisposing Factors and Morbidity. *Ophthalmology* **113**, 109-116.

Kim, J., Hegde, M. and Jayaraman, A. (2010) Co-culture of epithelial cells and bacteria for investigating host–pathogen interactions. *Lab Chip* **10**, 43-50.

ORIGINAL UNEDITED MANUSCRIPT

Downloaded from academic.oup.com/jambio/advance-article/doi/10.1093/jambio/lxag263/9013327 by guest on 11 November 2026

Kwong, S.M., Skurray, R.A. and Firth, N. (2004) *Staphylococcus aureus* multiresistance plasmid pSK41: analysis of the replication region, initiator protein binding and antisense RNA regulation. *Mol Microbiol* **51**, 497-509.

Lecuyer, S., Rusconi, R., Shen, Y., Forsyth, A., Vlamakis, H., Kolter, R. and Stone, H.A. (2011) Shear Stress Increases the Residence Time of Adhesion of *Pseudomonas aeruginosa*. *Biophys J* **100**, 341-350.

Mairey, E., Genovesio, A., Donnadieu, E., Bernard, C., Jaubert, F., Pinard, E., Seylaz, J., Olivo-Marin, J.-C., Nassif, X. and Duménil, G. (2006) Cerebral microcirculation shear stress levels determine *Neisseria meningitidis* attachment sites along the blood–brain barrier. *J Exp Med* **203**, 1939-1950.

Maki, K.L. and Ross, D.S. (2014) Exchange of Tears under a Contact Lens Is Driven by Distortions of the Contact Lens. *Integr Comp Biol* **54**, 1043-1050.

Marquart, M.E. (2011) Animal Models of Bacterial Keratitis. *Biomed Res Int* **2011**, 680642.

Masterton, S. and Ahearne, M. (2018) Mechanobiology of the corneal epithelium. *Exp Eye Res* **177**, 122-129.

Meacock, O.J. and Durham, W.M. (2023) Tracking bacteria at high density with FAST, the Feature-Assisted Segmenter/Tracker. *PLoS Comput Biol* **19**, e1011524.

Molladavoodi, S., Robichaud, M., Wulff, D. and Gorbet, M. (2017) Corneal epithelial cells exposed to shear stress show altered cytoskeleton and migratory behaviour. *PLoS ONE* **12**, e0178981.

Okurowska, K., Roy, S., Thokala, P., Partridge, L., Garg, P., MacNeil, S., Monk, P.N. and Karunakaran, E. (2020) Establishing a Porcine e*x vivo* Cornea Model for Studying Drug Treatments against Bacterial Keratitis. *J Vis Exp*, e61156.

ORIGINAL UNEDITED MANUSCRIPT

Downloaded from academic.oup.com/jambio/advance-article/doi/10.1093/jambio/lxag263/9013327 by guest on 11 November 2026

Palalay, J.-J.S., Simsek, A.N., Reed, J.L., Koch, M.D., Sabass, B. and Sanfilippo, J.E. (2023) Shear force enhances adhesion of *Pseudomonas aeruginosa* by counteracting pilus-driven surface departure. *Proc Natl Acad Sci USA* **120**, e2307718120.

Park, P.W., Pier, G.B., Hinkes, M.T. and Bernfield, M. (2001) Exploitation of syndecan-1 shedding by *Pseudomonas aeruginosa* enhances virulence. *Nature* **411**, 98-102.

Park, P.W., Pier, G.B., Preston, M.J., Goldberger, O., Fitzgerald, M.L. and Bernfield, M. (2000) Syndecan-1 Shedding Is Enhanced by LasA, a Secreted Virulence Factor of *Pseudomonas aeruginosa*. *J Biol Chem* **275**, 3057-3064.

Pedersen, R.M., Grønnemose, R.B., Stærk, K., Asferg, C.A., Andersen, T.B., Kolmos, H.J., Møller-Jensen, J. and Andersen, T.E. (2018) A Method for Quantification of Epithelium Colonization Capacity by Pathogenic Bacteria. *Front Cell Infect Microbiol* **8**, 16.

Pinnock, A., Shivshetty, N., Roy, S., Rimmer, S., Douglas, I., MacNeil, S. and Garg, P. (2017) *Ex vivo* rabbit and human corneas as models for bacterial and fungal keratitis. *Graefes Arch Clin Exp Ophthalmol* **255**, 333-342.

Putra, I., Rabiee, B., Anwar, K.N., Gidfar, S., Shen, X., Babalooee, M., Ghassemi, M., Afsharkhamseh, N., Bakhsh, S., Missiakas, D., Nezamabadi, A., Milani, B., Eslani, M. and Djalilian, A.R. (2019) *Staphylococcus aureus* alpha-hemolysin impairs corneal epithelial wound healing and promotes intracellular bacterial invasion. *Exp Eye Res* **181**, 263-270.

Rajas, O., Quirós, L.M., Ortega, M., Vazquez-Espinosa, E., Merayo-Lloves, J., Vazquez, F. and García, B. (2017) Glycosaminoglycans are involved in bacterial adherence to lung cells. *BMC Infect Dis* **17**, 319.

Rodesney, C.A., Roman, B., Dhamani, N., Cooley, B.J., Katira, P., Touhami, A. and Gordon, V.D. (2017) Mechanosensing of shear by *Pseudomonas aeruginosa* leads to increased levels of the cyclic-di-GMP signal initiating biofilm development. *Proc Natl Acad Sci USA* **114**, 5906-5911.

ORIGINAL UNEDITED MANUSCRIPT

Downloaded from academic.oup.com/jambio/advance-article/doi/10.1093/jambio/lxag263/9013327 by guest on 11 November 2026

732 Sanfilippo, J.E., Lorestani, A., Koch, M.D., Bratton, B.P., Siryaporn, A., Stone, H.A. and Gitai, Z.
733 (2019) Microfluidic-based transcriptomics reveal force-independent bacterial rheosensing.
734 *Nat Microbiol* **4**, 1274-1281.
735 Sarrazin, S., Lamanna, W.C. and Esko, J.D. (2011) Heparan sulfate proteoglycans. *Cold Spring*
736 *Harb Perspect Biol* **3**, a004952.
737 Schindelin, J., Arganda-Carreras, I., Frise, E., Kaynig, V., Longair, M., Pietzsch, T., Preibisch, S.,
738 Rueden, C., Saalfeld, S., Schmid, B., Tinevez, J.Y., White, D.J., Hartenstein, V., Eliceiri, K.,
739 Tomancak, P. and Cardona, A. (2012) Fiji: an open-source platform for biological-image
740 analysis. *Nat Methods* **9**, 676–682.
741 Srinivas, S.P., Mutharasan, R. and Fleiszig, S. (2002) Shear-induced ATP release by cultured
742 rabbit corneal epithelial cells. *Adv Exp Med Biol* **506**, 677–685.
743 Tan, S.Z., Walkden, A., Au, L., Fullwood, C., Hamilton, A., Qamruddin, A., Armstrong, M.,
744 Brahma, A.K. and Carley, F. (2017) Twelve-year analysis of microbial keratitis trends at a UK
745 tertiary hospital. *Eye (Lond)* **31**, 1229-1236.
746 Ting, D.S.J., Ho, C.S., Cairns, J., Elsahn, A., Al-Aqaba, M., Boswell, T., Said, D.G. and Dua, H.S.
747 (2021) 12-year analysis of incidence, microbiological profiles and *in vitro* antimicrobial
748 susceptibility of infectious keratitis: the Nottingham Infectious Keratitis Study. *Br J*
749 *Ophthalmol* **105**, 328-333.
750 Tremblay, Y.D.N., Vogeleer, P., Jacques, M. and Harel, J. (2015) High-Throughput Microfluidic
751 Method To Study Biofilm Formation and Host-Pathogen Interactions in Pathogenic
752 *Escherichia coli*. *Appl Environ Microbiol* **81**, 2827-2840.
753 Urwin, L., Okurowska, K., Crowther, G., Roy, S., Garg, P., Karunakaran, E., MacNeil, S.,
754 Partridge, L.J., Green, L.R. and Monk, P.N. (2020) Corneal Infection Models: Tools to
755 Investigate the Role of Biofilms in Bacterial Keratitis. *Cells* **9**, 2450.

ORIGINAL UNEDITED MANUSCRIPT

Downloaded from academic.oup.com/jambio/advance-article/doi/10.1093/jambio/lxag263/9013327 by guest on 11 November 2026

Vergunst, A.C., Meijer, A.H., Renshaw, S.A. and O'Callaghan, D. (2010) *Burkholderia cenocepacia* Creates an Intramacrophage Replication Niche in Zebrafish Embryos, Followed by Bacterial Dissemination and Establishment of Systemic Infection. *Infection and Immunity* **78**, 1495-1508.

Webster, S.S., Mathelié-Guinlet, M., Verissimo, A.F., Schultz, D., Viljoen, A., Lee, C.K., Schmidt, W.C., Wong, G.C.L., Dufrêne, Y.F. and O'Toole, G.A. (2022) Force-Induced Changes of PilY1 Drive Surface Sensing by *Pseudomonas aeruginosa*. *mBio* **13**, e03754-21.

WHO (2024) WHO Bacterial Priority Pathogens List, 2024: bacterial pathogens of public health importance to guide research, development and strategies to prevent and control antimicrobial resistance. https://www.who.int/publications/i/item/9789240093461.

Yu, Z., Hao, R., Du, J., Wu, X., Chen, X., Zhang, Y., Li, W., Gu, Z. and Yang, H. (2022) A human cornea-on-a-chip for the study of epithelial wound healing by extracellular vesicles. *iScience* **25**, 104200.

Author Contribution Statement:

L.U. and J.H.R.W. contributed equally to this work.

Lucy Urwin: Conceptualization, data curation, formal analysis, investigation, methodology, validation, writing- original draft, writing- review & editing.

James H. R. Wheeler: Data curation, formal analysis, investigation, methodology, validation, writing- original draft, writing- review & editing.

Paige A. Wolverson: Data curation, formal analysis, investigation, methodology, validation, writing – review and editing.

Luke R. Green: Funding acquisition, conceptualization, methodology, supervision, writing- review & editing.

Mahendra Raut: Methodology, validation, writing – review and editing.

Esther Karunakaran: Conceptualization, methodology, writing – review and editing.

ORIGINAL UNEDITED MANUSCRIPT

Downloaded from academic.oup.com/jambio/advance-article/doi/10.1093/jambio/lxag263/9013327 by guest on 11 November 2026

Lynda J. Partridge: Resources, supervision.

Peter N. Monk: Funding acquisition, conceptualization, project administration, supervision, writing- review & editing.

William M. Durham: Funding acquisition, methodology, project administration, resources, supervision, writing- review & editing.

Supporting Information:

All supplementary figures (**Fig. S1-S10**) and corresponding figure legends are contained in the Supporting Information.

Figures:

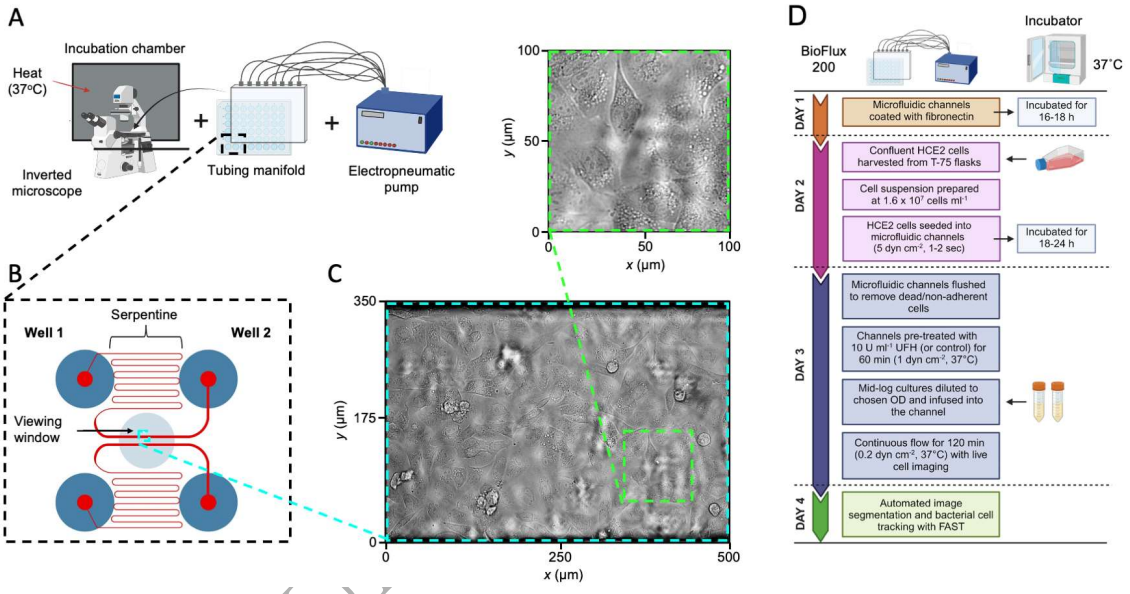


Figure 1. A microfluidic model to simulate bacterial keratitis. (A) The BioFlux microfluidic system uses a well plate containing 24 separate microfluidic channels connected to a computer-controlled pneumatic pump via a manifold. Microfluidic channels are imaged using an inverted fluorescent microscope fitted with an incubation chamber that maintains cells at 37°C. **(B)** Well 1 is connected to a long, narrow serpentine channel that leads to a wider test section before connecting to Well 2. While actual geometry is more complex, the schematic shown here illustrates the basic features of the device. **(C)** A confluent monolayer of human corneal epithelial cells (HCE2) in the 350 µm wide test section of

ORIGINAL MANUSCRIPT

Downloaded from academic.oup.com/jambio/advance-article/doi/10.1093/jambio/lxag263/9013327 by guest on 11 November 2026

the device. **(D)** Simplified workflow for studying the adhesion of bacteria to HCE2 monolayers. Panels A and D were created in BioRender: (A) Urwin, L. (2026) https://BioRender.com/p8x7605; (D) Urwin, L. (2026) https://BioRender.com/2kldh06. Panel B was generated using Vectorworks.

ALT-TEXT: 'Schematics, microscopy images and flow-chart illustrating a microfluidic experimental set-up for infecting corneal epithelial cells with pathogenic bacteria.'

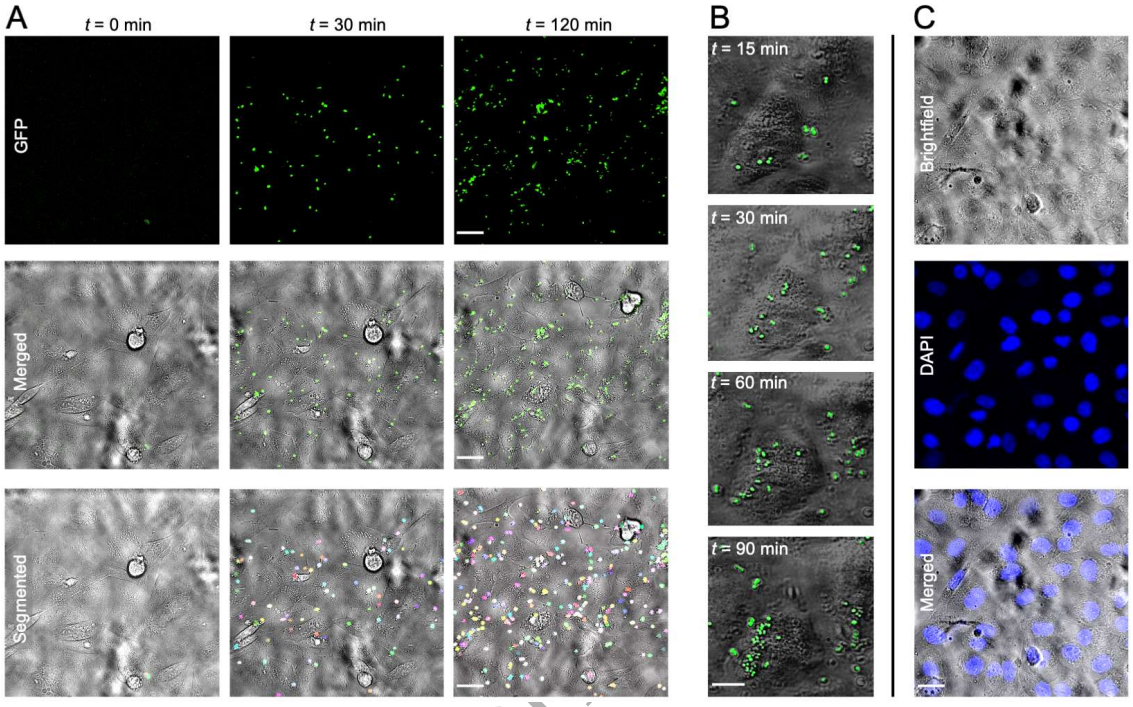


Figure 2. Bacterial infection of HCE2 monolayers under continuous fluid flow. HCE2 monolayers were infected with *S. aureus*, SH1000-GFP (green) for 120 min, under continuous flow conditions (0.2 dyn cm^{-2}) and imaged using fluorescence microscopy with a 20X **(A)** or 100X **(B)** objective. Individual bacterial cells were segmented and enumerated in 20X magnification fluorescence microscopy images using the Feature-Assisted Segmenter/Tracker software (FAST, (Meacock and Durham 2023)). **(C)** In separate experiments, HCE2 monolayers were cultured using the same conditions, fixed with 4% paraformaldehyde, stained with DAPI to label HCE2 nuclei, and imaged with a 20X objective. All scale bars are 20 μm.

ALT-TEXT: 'High-resolution microscopy images showing fluorescently labelled *Staphylococcus aureus* adhering to corneal epithelial cells under fluid flow.'

ORIGINAL UNEDITED MANUSCRIPT

Downloaded from academic.oup.com/jambio/advance-article/doi/10.1093/jambio/lxag263/9013327 by guest on 11 November 2026

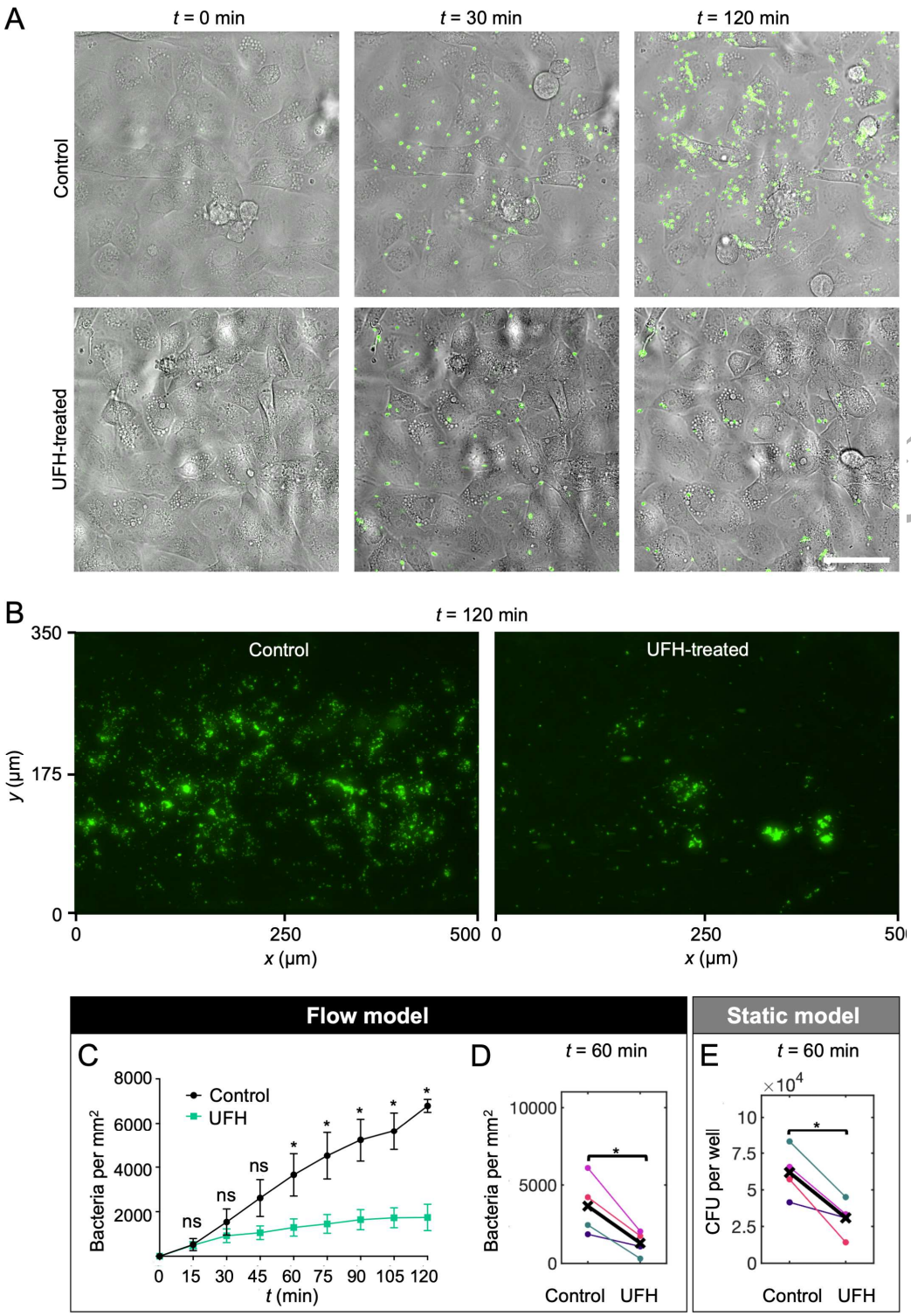


Figure 3. UFH reduces the adhesion of *S. aureus* to corneal epithelial cells in both the presence and absence of flow. (A) HCE2 monolayers were pre-treated with live cell imaging solution (LCIS) containing 10 U ml^{-1} unfractionated heparin (UFH), or LCIS without UFH (control). These monolayers

Downloaded from academic.oup.com/jambio/advance-article/doi/10.1093/jambio/lxag263/9013327 by guest on 11 November 2026

were then infected with *S. aureus*, SH1000-GFP (green) for 120 min in the presence of continuous flow (0.2 dyn cm^{-2}). Scale bar is 50 µm. **(B)** The maximum intensity projection of a series of fluorescent images captured using a 20X objective at different z-elevations spanning 25 µm. **(C)** The numerical density of *S. aureus* bacteria attached to HCE2 cells was quantified in four separate experiments (n=4), which compare bacterial attachment to HCE2 cells pre-treated with UFH to that of a control in a separate microfluidic channel. Data from two separate fields of view were combined for each biological repeat. Error bars show mean of biological repeats ± SEM. A paired *t*-test was used to compare the treatment and control at each timepoint and timepoints where the treatment was statistically different from the control ($p \leq 0.05$) are marked with an asterisk, whereas ns denotes timepoints where the difference was not significant. Data for each individual timepoint is shown in **Fig. S5**. **(D)** The numerical density of bacteria at 60 min post-infection for each of the microfluidic experiments shown in C ($p = 0.0391$, paired *t*-test). **(E)** Separate experiments in the absence of fluid-flow were also conducted using 96-well plates where HCE2 monolayers were either pre-treated with KSFM media containing 10 U ml^{-1} unfractionated heparin (UFH) or a KSFM-only control. Cells were then infected with *S. aureus* for 60 min under static conditions. Adherent bacteria were enumerated 60 min post-infection. Mean values from four biological repeats are shown (n=4), each of which contains three technical replicates. A paired *t*-test indicated UFH significantly reduces bacterial adhesion in these static conditions ($p = 0.0226$). In D and E, thin coloured lines connect the paired UFH-treated and control measurements from each biological replicate, whilst the thick black line shows the mean across all four biological replicates.

ALT-TEXT: 'High-resolution microscopy images and graphs quantifying the attachment of *Staphylococcus aureus* to corneal epithelial cells with and without UFH treatment.'

ORIGINAL UNEDITED MANUSCRIPT

Downloaded from academic.oup.com/jambio/advance-article/doi/10.1093/jambio/lxag263/9013327 by guest on 11 November 2026

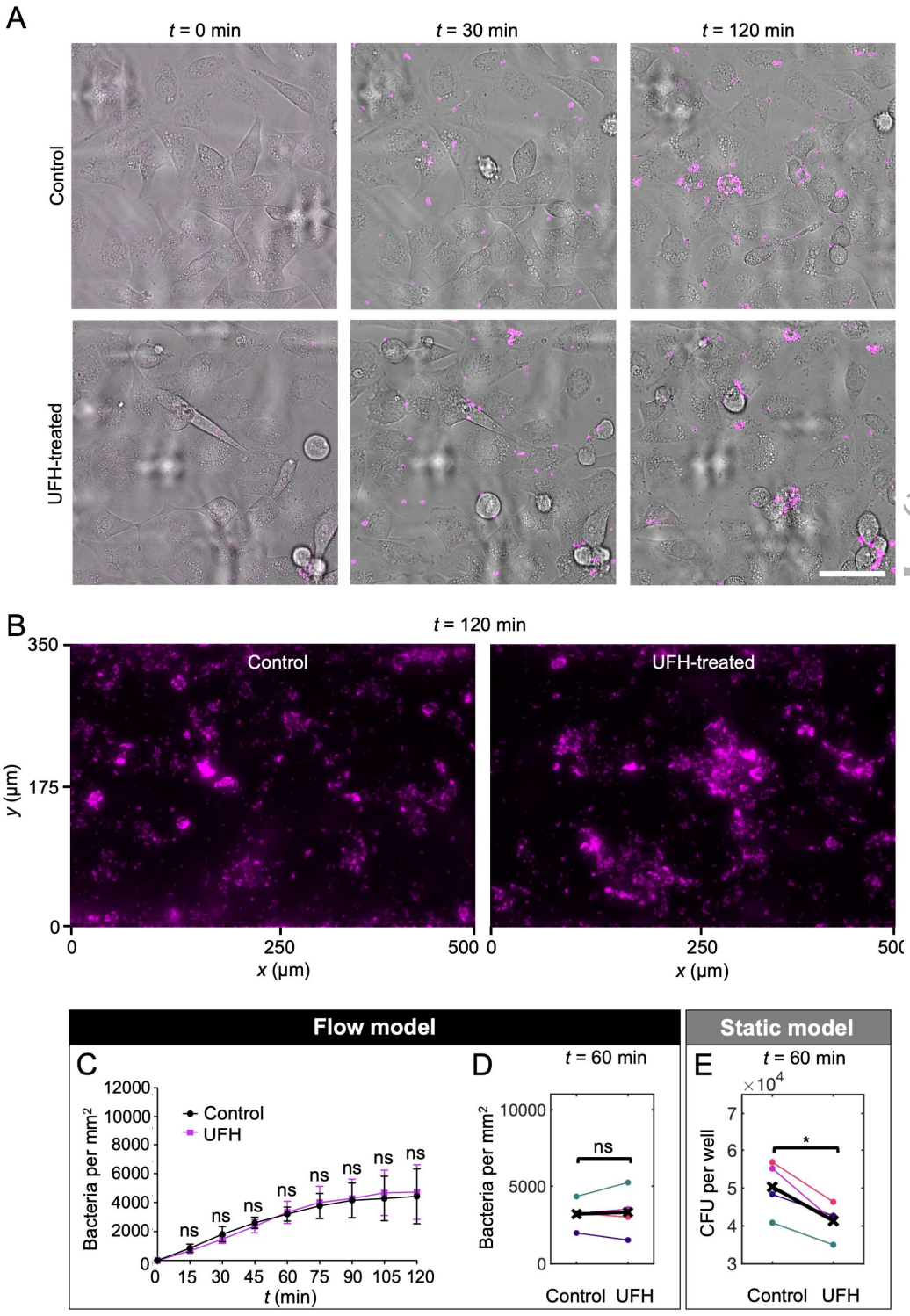


Figure 4. Pre-treatment of HCE2 monolayers with UFH reduces *P. aeruginosa* adhesion in static conditions but has no appreciable effect in a microfluidic assay where flow is present. (A) HCE2 monolayers were pre-treated with live cell imaging solution (LCIS) containing 10 U ml^{-1} UFH, or LCIS without UFH (control). These monolayers were then infected with *P. aeruginosa*, PAO1-GFP (magenta)

Downloaded from academic.oup.com/jambio/advance-article/doi/10.1093/jambio/lxag263/9013327 by guest on 11 November 2026

for 120 min in the presence of continuous flow (0.2 dyn cm^{-2}). Scale bar is 50 µm. **(B)** The maximum intensity projection of a series of fluorescent images captured using a 20X objective at different z-elevations spanning 25 µm. **(C)** The numerical density of *P. aeruginosa* bacteria attached to HCE2 cells was quantified in four separate experiments (n=4), which compare bacterial attachment to HCE2 cells pre-treated with UFH to that of a control in a separate microfluidic channel. Data from two separate fields of view were combined in each biological repeat. Error bars show mean of biological repeats ± SEM. A paired t-test was used to compare the treatment and control at each timepoint, ns denotes timepoints where the difference was not significant. Data for each individual timepoint is shown in **Fig. S9**. **(D)** The numerical density of bacteria at 60 min post-infection for each of the microfluidic experiments shown in C (p= 0.7182, paired t-test). **(E)** Separate experiments in the absence of fluid-flow were also conducted using 96-well plates where HCE2 monolayers were either pre-treated with KSFM media containing 10 U ml^{-1} unfractionated heparin (UFH) or a KSFM-only control. Cells were then infected with *P. aeruginosa* for 60 min under static conditions. Adherent bacteria were enumerated 60 min post-infection. Mean values from four biological repeats are shown (n=4), with combined data from three technical replicates per biological repeat. A paired t-test indicated UFH significantly reduced bacterial adhesion in these static conditions (p= 0.0200). In D and E, thin coloured lines connect the paired UFH-treated and control measurements from each biological replicate, whilst the thick black line shows the mean across all four biological replicates.

ALT-TEXT: 'High-resolution microscopy images and graphs quantifying the attachment of *Pseudomonas aeruginosa* to corneal epithelial cells with and without UFH treatment.'

ORIGINAL UNEDITED MANUSCRIPT

Downloaded from academic.oup.com/jambio/advance-article/doi/10.1093/jambio/lxag263/9013327 by guest on 11 November 2026